

## ESTIMATION OF ULTRA WIDE BAND CHANNEL DEGREES OF FREEDOM

RACHID SAADANE\* and DRISS ABOUTAJDINE†  
*LRIT-GSCM, Member of the Académie,  
 Hassan II des Sciences et Techniques, Faculty Sciences,  
 Mohammed V-Agdal University,  
 av. Ibn Battouta, BP 1014., Rabat, Morocco*  
 \**rachid.saadane@gmail.com*  
 †*aboutaj@fsr.ac.ma*

AAWATIF MENOUNI HAYAR‡ and RAYMOND KNOPP§  
*Eurecom Institute,  
 BP 193,F-06904 Sophia Antipolis cedex, France*  
 ‡*aawatif.menouni@eurecom.fr*  
 §*raymond.knopp@eurecom.fr*

Accepted 17 April 2007

Multipath propagation effects encountered in mobile wireless channels provide additional degrees of freedom [Ganesan *et al.*, 2000] that can be exploited via appropriate signaling and reception. In this work, based on a set of measurements conducted at Eurecom, we consider a novel approach of analyzing an Ultra Wide Band (UWB) indoor radio propagation channel by performing an eigen-decomposition and observing the scaling of the number of significant eigenvalues with the channel bandwidth by using the *Akaike information criterion* (AIC) and *Minimum Description Length* (MDL). These criterion are applied to estimate the number of degrees of freedom (DoF) of an UWB in an indoor environment. We evaluate our approach under both scenarios, line-of-sight (LOS) and non-line-of-sight (NLOS). Based on AIC and the MDL criterion, we find that this number is large; this has important consequences on the receiver design. We show also, that in opposition to the accepted idea in the literature, the number of Degrees of Freedom (DoF) does not increase linearly with the channel bandwidth. Hence, the results of the estimation of UWB channel entropy confirm that the number of DoF increases sub-linearly with the channel bandwidth.

*Keywords:* UWB channel measurements; degrees of freedom; empirical entropy.

2 *R. Saadane et al.*

## 1. Introduction

UWB systems are now emerging across a variety of commercial and military applications, including communications, radar, geolocation, and medical applications, in [Alomainy *et al.*, 2006], the UWB signals present good penetrating properties that could be applied to imaging in medical applications. First generation commercial wireless UWB products are anticipated to be widely deployed. This has been fueled by a demand for high frequency utilization and a large number of users requiring simultaneous multi-dimensional, to allow the user to transmit and receive two or more unique data streams through one radio channel, high data rate access for applications of wireless internet and e-commerce.

UWB systems are often defined to have a relative bandwidth that is larger than 20% and/or an absolute bandwidth of more than 500 MHz [FCC, 2002]. The UWB systems using large absolute bandwidth, are robust to frequency-selective fading, which has significant implications on both, design and implementation. Among the important characteristics of the UWB technology are low power devices, accurate localization, a high multipath immunity, low complexity hardware structures and carrier-less architectures [Win *et al.*, 1998]. Additionally, the spreading of the information over a very large frequency range decreases the spectral density and makes it compatible with existing systems.

For designing and implementing any wireless system, channel sounding and modeling are a basic necessity. Several studies, theoretical and practical, have shown an extreme difference with respect to narrowband channels [Cassoli *et al.*, 2002; Kunisch *et al.*, 2002].

The capacity of multipath channel in the limit of infinite bandwidth is identical to the capacity of the Additive White Gaussian Noise (AWGN) channel:

$$\lim_{B \rightarrow \infty} \log_2 \left( 1 + \frac{P}{BN_0} \right) = \frac{P}{N_0} \log_2(e), \quad (1)$$

where  $P$  is the received power and  $N_0$  is the one sided noise spectral level. Golay [Golay, 1949], shows that this capacity, with non-fading channels, can be approached by On-Off keying (pulse position modulation) with low duty cycle. Also, Telatar and Tse [Telatar *et al.*, 2000] show that: With spectrum signals over multipath channels, the data rate is inversely proportional to the number of channel paths. In the direct sequence spread spectrum without duty cycle system the throughput tends to zero in the limit if the number of multipaths increases. The question here is that: **How the number of multipaths increases with the channel bandwidth?**

When the bandwidth increases, the temporal resolution increases, this allows us to discover the hidden paths, but beyond a given bandwidth all the independent paths are resolved (the new resolvable paths are mostly dependent to the ones already resolved). Physically the growth of number of multipaths with channel bandwidth can be explained as follow: The number of multipaths increases with the bandwidth because the reflection (due to constitutive parameters) and diffraction mechanisms are frequency and bandwidth dependent. To evaluate the number of paths in a given environment that corresponds a sitting (LOS or NLOS) for a given bandwidth, we use DoF (representing the number of independent paths) that is based on the eigen decomposition of channel covariance matrix (to extract the independent components in the channel i.e. independent paths).

The goal of this contribution is to analyze the impact of these extremely large systems bandwidth on the covariance matrix channel. We are primarily interested in assessing the

growth in the number of DoF needed to characterize the channel as a function of the system bandwidth using the AIC and the MDL. We are also interested in the root mean square (*rms*) delay spread behavior for a given threshold of received power (98% in the total received energy) as a function of the system bandwidth for both LOS and NLOS cases. To assess the channel uncertainty, the well known channel entropy parameter is evaluated empirically.

The remaining of the paper is organized as follows. Section 2 describes the channel covariance matrix. In Sec. 3 we outline the covariance matrix estimation and the two information theoretic criteria: the AIC and the MDL methods used for estimating the number of DoF of the UWB propagation channel. Section 4 describes briefly the channel measurements based in this work, Sec. 5 presents the numerical results about the number of DoF, the (*rms*) delay spread and the empirical channel entropy. Finally Sec. 6 presents the conclusions of this study.

## 2. The Channel Covariance Matrix Formulation

The radio-propagation channel is randomly time-varying due to variations in the environment and mobility of transmitters and receivers. It is classically represented, following the work of Bello [Bello *et al.*, 1963; 1964] by its input delay-spread function  $h(t, \tau)$  well known the time-varying Channel Impulse Response (CIR). The variable  $t$  in the CIR notation represents the time-varying behavior of the channel caused by the mobility of either the transmitter, the receiver or the scatterers. The second variable  $\tau$  represents the delay domain in which we characterize the channel regarding the most important arriving paths. We consider for each measurement a fixed position at the transmitter and the receiver sides, and a static environment (at least during the time-frame of one measurement). We are thus considering a static channel and we can then simplify the notation of the CIR by dropping its dependence on  $t$ .

Let

$$\mathbf{h} = [h_{W,1}, h_{W,2}, \dots, h_{W,N}]^T \quad (2)$$

be the matrix containing the  $N$  different impulse response for the  $N$  different antenna configurations, where  $h_{W,i}$  is expressed as

$$h_{W,i} = g_{W,i} + n_{W,i}, \quad i = 1, \dots, N, \quad (3)$$

where  $n_{W,i}$  is zero-mean additive white Gaussian noise with power spectral density equal to  $\sigma_n^2$  at all frequencies in the bandwidth of interest. We neglect any nonlinear perturbation caused by measurement elements (e.g. vector network analyzer (VNA) amplifiers), which were treated in a more general setting in [Matz *et al.*, 2002]. We include the frequency response of the antenna as part of the channel response as argued in [Saadane *et al.*, 2004], and moreover, the linear response of the equipment is assumed to be perfectly accounted for in the calibration of the measurement apparatus. The noise process, resulting from thermal noise in the receive chain of the VNA and the noise generated by device itself, is assumed to be white in the band of interest. We therefore have that

$$\mathbf{g} = [g_{W,1}, g_{W,2}, \dots, g_{W,N}] \quad (4)$$

are the observations of the noise-free channel process corresponding to  $N$  observation positions.

4 *R. Saadane et al.*

Due to the rapid variation of the wave's phase (from 0 to  $2\pi$  over one wavelength), we can assume that the received electric field at each position represents a zero-mean process, and thus  $g(t)$  is taken to be zero-mean. We remark that this does not rule out the possibility of line-of-sight propagation as will be treated shortly. The VNA provides samples of the observed channel process in the frequency domain,  $H(k\Delta f)$ , where  $\Delta f$  is the frequency separation, in our case 1 MHz. Furthermore, it is a filtered version of the channel response, where the filter corresponds to an ideal bandpass filter of bandwidth  $W$  centered at

$$f_c = \frac{f_{\max} - f_{\min}}{2}. \quad (5)$$

After removing the carrier frequency  $f_c$ , we denote the complex baseband equivalent filtered channel by  $h_W$ . By sampling the frequency response in the VNA we obtain an aliased version of  $h_W$  denoted by

$$\tilde{h}_W(t) = \sum_k h_W(t - k/\Delta f). \quad (6)$$

The time-domain samples obtained by performing an inverse discrete Fourier transform (IDFT) on the vector

$$\mathbf{H} = (H(0) H(\Delta f) \dots H((N-1)\Delta f))^T \quad (7)$$

are samples of  $\tilde{h}_W(t)$  at sampling frequency  $W$  Hz. We note that the choice of frequency separation  $\Delta f$  has an impact on how closely  $\tilde{h}_W(t)$  approximates  $h_W(t)$  in the interval  $[0, 1/\Delta f)$ . In our case the choice of  $\Delta f = 1$  MHz guarantees that the approximation will be very accurate since the typical delay spread of the considered channels is less than 100 ns. Therefore time-domain aliasing will not distort the channel measurement. For this reason we assume in what follows that the measurement equipment provides perfect samples of  $h_W(t)$ .

Our approach to characterize the UWB propagation channel is based on the analysis of the channel subspace and the eigen-decomposition of the covariance matrix,  $\mathbf{K}_h$ , of the samples of  $h_W(t)$ , denoted by the vector

$$\mathbf{h} = \left( h_W(0) h_W\left(\frac{1}{W}\right) \dots h_W\left(\frac{p-1}{W}\right) \right)^T, \quad (8)$$

where  $p$  is the length of the channel used for statistical analysis with  $0 \leq p \leq \frac{1}{\Delta f} - \frac{1}{W}$ . This allows us to estimate the number of DoF characterizing  $h_W(t)$  [Slepian *et al.*, 1961]. A similar approach for estimating the (finite) unknown number of Gaussian signals using a finite set of noisy observations is described in [Wax *et al.*, 1985; Williams *et al.*, 1994]. These techniques amount to determining the finite dimension of the signal subspace. In order to estimate the true covariance matrix  $\mathbf{K}_h$ , we use statistical averages based on observations from  $(20 \times 50)$  positions, 20 transmitter positions, 50 receiver positions for each transmitter position.

### 3. Estimation of the Number of Degrees of Freedom

#### 3.1. Covariance matrix estimation

The sample covariance matrix is a maximum-likelihood estimate, under the assumption of a large number of independent channel observations [Anderso *et al.*, 1984] which arise

from the different transmitting and receiving antenna positions as explained earlier. The separation between positions on the grids must be large enough to obtain sufficient variation of the wave's phase,  $\Delta\phi$ ,<sup>a</sup> in order to extract all the DoF of the channel. On the other hand, the separation must be small enough to ensure that the distance between transmitter and the receiver (6 meters in our primary measurement scenario) remains virtually constant. If both constraints are satisfied we can assume that  $\mathbf{K}_h$  will depend solely on the slowly-varying parameters (distance, arrival angles, scatterers, geometrical settings, ...) and thus will not vary significantly across the set of the total transmitter and receiver positions.

The multipath indoor radio propagation channel is normally modeled as a complex lowpass equivalent impulse response given by

$$h(t) = \sum_{l=0}^{L-1} a_l p_l(t - \tau_l), \quad (9)$$

where  $L$  is the number of multipath components, and  $a_l = |a_l|e^{j\theta_l}$  and  $\tau_l$  are the complex attenuation and propagation delay of the  $l$ th path, respectively, while the multipath components are indexed so that the propagation delays  $\tau_l$ ,  $0 \leq k \leq L-1$  are in ascending order. As a result,  $\tau_0$  in the model denotes the propagation delay of direct Line-of-Sight.

For simplifying the problem we make  $p(t) = \delta(t)$ , where  $\delta$  denote Dirac function. Taking the Fourier transform of (9), the frequency-domain channel response can be expressed as

$$H(f) = \sum_{l=0}^{L-1} a_l e^{-j2\pi f \tau_l}. \quad (10)$$

The covariance matrix of measured channel samples,  $\mathbf{h}$ , is written as

$$\mathbf{K}_h = E[\mathbf{h}\mathbf{h}^H] = E[\mathbf{g}\mathbf{g}^H] + \sigma_n^2 \mathbf{I}, \quad (11)$$

where  $\mathbf{g}$  is a vector of samples of the noise-free channel process, and  $\mathbf{I}$  is the identity matrix. The maximum-likelihood covariance matrix estimate  $\mathbf{R}$  computed from  $N$  statistically independent channel observation with length  $p$  and  $p < N$  is given by [Anderso *et al.*, 1984]

$$\mathbf{R} = \mathbf{K}_h^N = \frac{1}{N} \sum_{i=1}^N \mathbf{h}_{W,i} \mathbf{h}_{W,i}^H. \quad (12)$$

The assumption of  $p < N$  holds in our case since we ensure that the length of sampled CIR is less than 500 samples which represents the total number of channel observations for one scenario. For small  $d/\lambda$ , the assumption of independent observations and thus that the channel samples are spatially decorrelated is justified in an indoor Multiple Input Multiple Output (MIMO) setting in [Svantesson *et al.*, 2002]. In the context of our measurements, the multiple transmitter/receiver grid can equivalently be seen as a large(50×20) MIMO system.

---

<sup>a</sup> $\Delta\phi = \frac{2\pi d}{\lambda}$  is the wave's phase variation between two positions,  $d$  is the corresponding distance and  $\lambda$  is the wavelength varying from 3 to 10 cm for a UWB channel bandwidth ranging from 3 to 10 GHz.

6 *R. Saadane et al.*

### 3.2. Information theoretic criteria

AIC and MDL are model-order determination algorithms that can also be used for determining how many signals are present in vector valued data. Suppose the  $M \times 1$  complex vector  $h(t)$  can be modeled as

$$h(t) = As(t) + n(t), \quad (13)$$

$A$  is a rank( $P$ )  $M \times P$  complex matrix whose columns are determined by the unknown parameters associated with each signal.  $s(t)$  is a  $P \times 1$  complex vector whose  $p$ th element is the waveform of the  $p$ th signal, and  $n(t)$  is a complex, stationary, and ergodic Gaussian process with zero mean and covariance matrix  $E\{n(t)n'(t)\} = \sigma_n^2 I_n$ . The problem is to determine  $P$  from  $N$  observations of  $h(t)$ ; i.e.,  $h(t_1), \dots, h(t_N)$ . Let

$$\mathbf{R} = E\{h(t)h'(t)\} \quad (14)$$

be the covariance matrix of the data  $h(t)$ , and

$$\hat{\mathbf{R}} = \frac{1}{N} \sum_{i=1}^N h(t_i)h'(t_i), \quad (15)$$

where  $\hat{\mathbf{R}}$  is an estimate of  $\mathbf{R}$ .

The covariance matrix is Hermitian and positive definite. For this reason, an unitary matrix  $\mathbf{U}_h$  exists such that the Karhunen-Loève (KL) expansion gives [Van Trees, 2001]

$$\mathbf{R} = \mathbf{U}_h \Lambda_h \mathbf{U}_h^H = \sum_{i=1}^N \lambda_i(\mathbf{h}) \psi_i(\mathbf{h}) \psi_i^H(\mathbf{h}); \quad \mathbf{U}_h^H \mathbf{U}_h = \mathbf{I}_N, \quad (16)$$

where  $\lambda_1(\mathbf{h}) \geq \lambda_2(\mathbf{h}) \geq \dots \geq \lambda_N(\mathbf{h})$ ,  $\psi_i(\mathbf{h})$  is the  $i$ th column of  $\mathbf{U}_h$  and  $\mathbf{I}_N$  is the  $N \times N$  identity matrix with  $N$  number of samples.  $\lambda_i(\mathbf{h})$  and  $\psi_i(\mathbf{h})$  are the  $i$ th eigenvalues and eigenvectors of  $\mathbf{R}$ , respectively.

Furthermore, if  $P$  uncorrelated signals are present, the  $M - P$  smallest eigenvalues of  $\mathbf{R}$  are all equal to the noise power  $\sigma_n^2$ , and the vector of parameters  $\Theta^{(P)}$  specifying  $\mathbf{R}$  can be written as

$$\Theta^{(P)} = [\lambda_1, \lambda_2, \dots, \lambda_{P-1}, \lambda_P, \sigma_n^2, \psi_1^T, \psi_2^T, \dots, \psi_P^T]. \quad (17)$$

The number of signals are determined from the estimated covariance matrix  $\hat{\mathbf{R}}$ . In [Wax *et al.*, 1985] the AIC criteria was adapted for detection of the number of signals. This procedure is recalled here in simplified form.

If  $\hat{\lambda}_1, \hat{\lambda}_2, \dots, \hat{\lambda}_M$  are the eigenvalues of  $\hat{\mathbf{R}}$  in the decreasing order then

$$AIC(k) = -2 \log \left( \frac{\prod_{i=k+1}^p \hat{\lambda}_i(\mathbf{h})^{\frac{1}{(p-k)}}}{\frac{1}{p-k} \sum_{i=k+1}^p \hat{\lambda}_i(\mathbf{h})} \right)^{N(p-k)} + 2k(2p - k), \quad (18)$$

and

$$MDL(k) = -\log \left( \frac{\prod_{i=k+1}^p \hat{\lambda}_i(\mathbf{h})^{\frac{1}{(p-k)}}}{\frac{1}{p-k} \sum_{i=k+1}^p \hat{\lambda}_i(\mathbf{h})} \right)^{N(p-k)} + \log(N) \frac{k(2p - k + 1)}{4}. \quad (19)$$

The number of DoF, possibly the number of significant eigenvalues, is determined as the value of  $k \in \{0, 1, \dots, p - 1\}$  which minimizes the value of (18) or (19). In this work, the

number of DoF represents the number of unitary dimension independent channels that constitute an UWB channel.

#### 4. UWB Channel Measurement

In this section, we present and analyze the results obtained from the UWB channel measurement conducted at Eurecom Institute [Saadane *et al.*, 2004].

The measurements were performed in the frequency domain using a Vector Network Analyzer (Rohde and Schwarz, ZVM family). From these measurements we determine the complex channel transfer function  $H(f)$ . The measured frequency range was 3 to 9 GHz, this leads a delay resolution of approximately 0.16 ns. The spectrum was divided into 6003 points i.e. 1 MHz frequency sampling step. The antenna separation is 6 meters and the measurements were peer-to-peer. Also the channel response include the antenna effects. In following section we present scenarios description and data analysis and post-processing.

##### 4.1. Scenarios description

The results and the analysis in this paper were based on measurement channel produced as a result of the LOS and NLOS scenario carried out at Mobile Communications Laboratory. All these measurement are realized over 6 GHz bandwidth, for all locations both the transmit and receive antennas remained fixed at equal heights (1.5 meters). Figure 1 shows the general architectural of the room where the used measurements data in this work are taken. From this figure we see that the transmitter position is indicated by Tx and the receiver location is indicated by Rx.

##### 4.2. Data analysis and post-processing

Before any statistical channel process can be carried out, in first time we appropriate data analysis technique in order to extract the channel parameters of interest from measurement

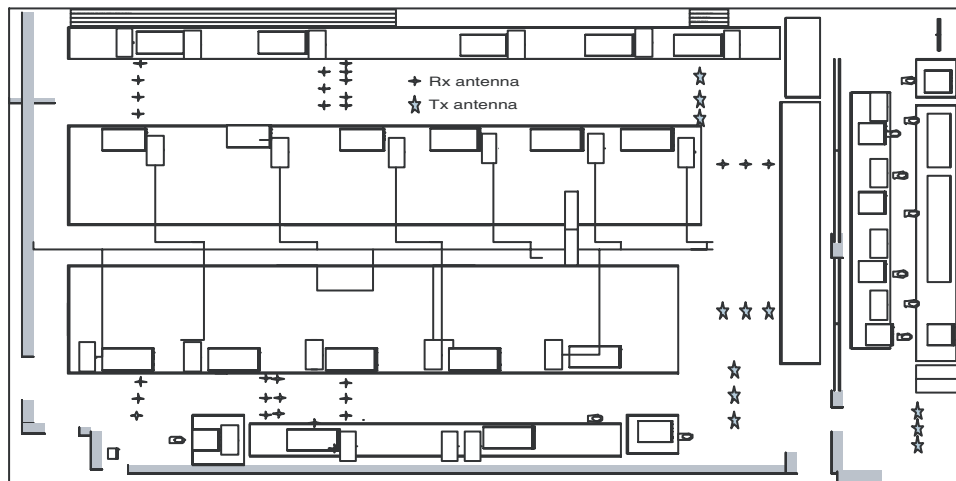


Fig. 1. Layout of one location where the channel measurements are conducted.

8 *R. Saadane et al.*

data, using Matlab. The data analysis procedures are organized as follow:

- (1) Since the VNA provides the measure of the channel (including the effects of the cables and the connectors), in order to remove these elements effect, a calibration procedure is needed.
- (2) Assuming that the channel is quasi-static, averaging is carried out over the temporal domain for each block of channel transfer function at each point in the space (for example grid of measurement  $20 \times 50$  i.e. 20 transmitter position over 50 receiver position). this assumption is justified by since no movement was allowed during the measurement only the manipulator in the environment of measurement.
- (3) Frequency windowing was applied prior to the transformation from the frequency domain the time domain. In this work the Hamming window is chosen.
- (4) The windowed channel transfer functions were transformed to the Channel Impulse Responses (CIRs) by using the Inverse Fast Fourier Transform (IFFT).
- (5) The channel impulse responses are normalized such that the total power in each power delay profile is equal to one.

## 5. DoF and Entropy Results

### 5.1. DoF evaluation

Figure 2 (resp. Fig. 3) considers LOS (resp. NLOS) measurements settings, we plot the AIC and MDL functions for two different bandwidths typically 200 MHz and 6 GHz. The minimum of AIC or MDL curves give the number of significant eigenvalues. As a matter of fact, we see that the number of DoF increases with bandwidth but not linearly, Table 1 summarized some value of  $k$  that minimize the AIC and MDL criterion. Thus, for 200 MHz bandwidth, we capture 98% of the energy with 29 significant eigenvalues whereas for 6 GHz channel bandwidths the number of eigenvalues is 50.

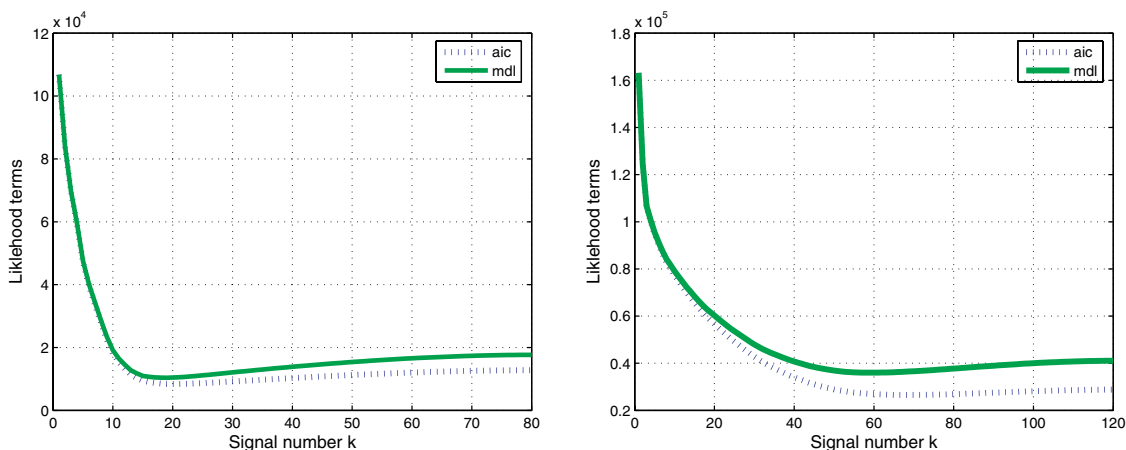


Fig. 2. The min of AIC and MDL curves corresponds to the number of DoF for 200 MHz (Left) and 6 GHz (Right) for LOS case.

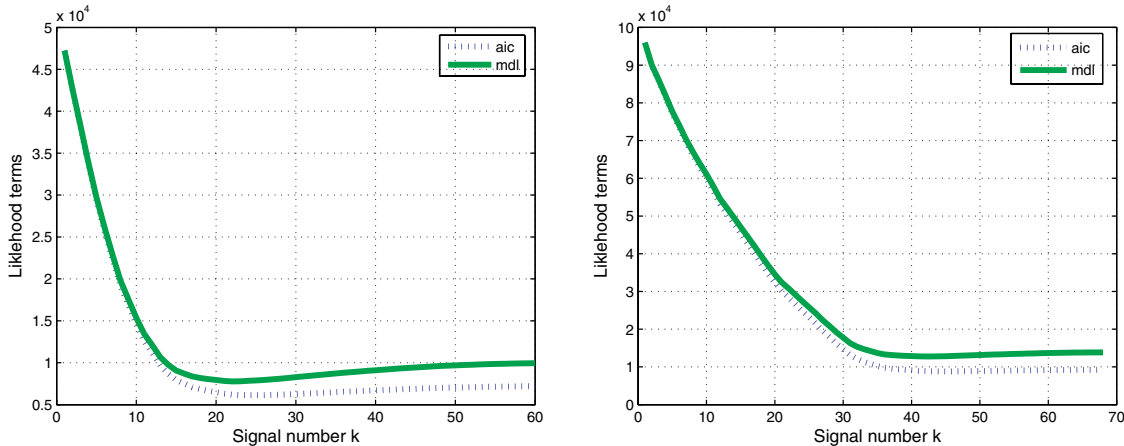


Fig. 3. The min of AIC and MDL curves corresponds to the number of DoF for 200 MHz (Left) and 6 GHz (Right) for NLOS. case.

Table 1. The values of  $k$  minimize AIC and MDL criteria.

$\Delta W$	Settings			
	LOS		NLOS	
	200 MHz	6 GHz	200 MHz	6 GHz
$k_{AIC}$	23	68	25	46
$k_{MDL}$	21	60	23	42

To illustrate the relationship between number of (DoF) and system bandwidth, we recall that for a signal with duration  $T$  and frequency band  $\Delta W$ , the number of DoF of the signal space  $N_{dof}$  is given by [Gallagher, 1968]:

$$N_{dof} = T \cdot \Delta W + 1. \quad (20)$$

According to [Ganesan *et al.*, 2000], if we find that if one transmits a band limited and time limited signal over a fading channel with *rms* delay spread  $T_d$ , the channel (DoF)  $N$  is approximately given by:

$$N = T_d \cdot \Delta W. \quad (21)$$

The APDP is characterized by the first central moment (mean excess delay)  $\tau_m$  and the square root of the second moment of the APDP root mean square  $\tau_{rms}$  delay spread. Using the traditional definitions as found in [Rappaport *et al.*, 1999], delay spread is given by:

$$\tau_{rms} = \sqrt{\frac{\sum_{i=1}^N (\tau_i - \tau_m)^2 |h(\tau_i)|^2}{\sum_{i=1}^N |h(\tau_i)|^2}}. \quad (22)$$

To investigate deeply the validity of this relationship for UWB channels, we measure the evolution of the  $\tau_{rms}$  delay spread with the frequency bandwidth, for both LOS and

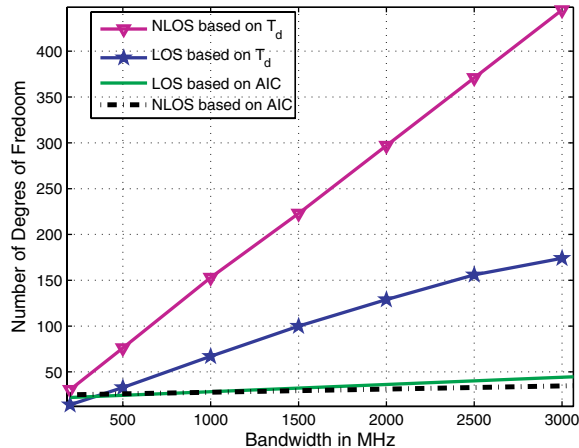


Fig. 4. Evolution of the number of DoF for LOS and NLOS cases.

NLOS cases, for one fixed threshold of received energy  $-20$  dB attenuation regarding the first arriving path. Then we plot, on Fig. 4, the computed number of DoF following equation (21) and compare this from measurements.

We then compare this result with the number of (DoF) obtained by AIC criterion from measurements. For 98% of the captured energy, we notice that the number of eigenvalues using the relationship in (21) increases linearly with the bandwidth for both LOS and NLOS case. In opposition, the number of eigenvalues calculated directly from measurements by AIC tends towards saturation beyond 2000 MHz frequency bandwidth for LOS case and beyond 1500 MHz frequency bandwidth for NLOS case.

## 5.2. Empirical entropy evaluation

The entropy is a measure of disorder of a system. Our system is the UWB channel and the disorder concerns the independent paths in this channel. As discussed above  $\hat{R}$  is the estimated covariance matrix,  $\hat{\lambda}_k$  is the  $k$ th eigenvalues of  $\hat{R}$  and  $\sum_k \hat{\lambda}_k = 1$ . In [Tsuda *et al.*, 2004] the Von Neumann entropy is given by

$$E(K) = -\text{tr}[\hat{R} \log \hat{R}], \quad (23)$$

in this work, the Von Neumann Entropy presents the Shannon entropy of eigenvalues.

Let  $\hat{S}$  the empirical entropy

$$\hat{S} = -\text{tr}[\hat{R} \log \hat{R}] = -\sum_{k=1}^L \hat{\lambda}_k \log \hat{\lambda}_k, \quad (24)$$

we call  $\hat{S}$  empirical entropy because it is calculated based on estimated eigenvalues from a given set of channel measurements.

To confirm the results presented previously in the channel DoF saturation versus the channel bandwidth. We evaluate the channel entropy  $\hat{S}$  for both LOS and NLOS settings.

In Fig. 5, the channel entropy  $\hat{S}$  is plotted for both LOS and NLOS scenarios with respect to the channel frequency band width. From this figure, we can see that the  $\hat{S}$

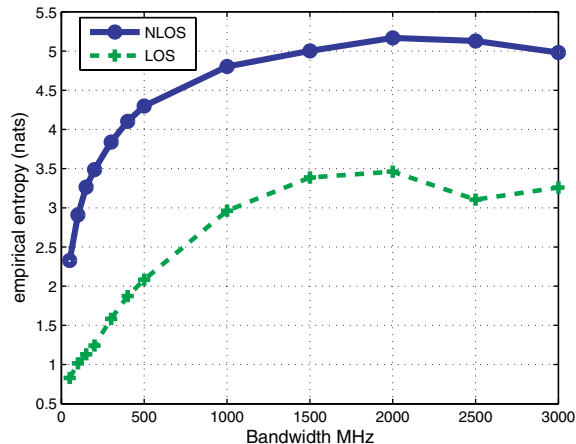


Fig. 5. The empirical entropy evolution versus channel bandwidth for LOS and NLOS cases.

Table 2. The delay spread versus band width  $\Delta W$ .

$\Delta W$	Delay Spread ( <i>ns</i> )			
	-10 dB threshold		-20 dB threshold	
	LOS	NLOS	LOS	NLOS
200 MHz	25	45	73	99
500 MHz	20	41	44	71
1000 MHz	15	40	41	70
1500 MHz	10	39	40	68
2000 MHz	9	39	37	68
2500 MHz	9	38	37	68
3000 MHz	9	38	37	68

under NLOS case is greater than the  $\hat{S}$  found under LOS one. This result confirms that the uncertainty increases with NLOS conditions which is due to the generation of supplementary multipaths under this environment. Figure 5 shows also that, the channel entropy  $\hat{S}$  increases with the frequency bandwidth but not linearly which confirms the saturation and the sub-linear behavior observed previously of the DoF.

## 6. Conclusion

In this work, we have used AIC and MDL criteria to estimate the number of DoF of an UWB channel in an in-door environment. We have also studied the evolution of the rms delay spread behavior,  $T_d$ , as a function of frequency bandwidth based on measurements campaigns carried out at Eurecom Mobile Communication Laboratory. We have also compared the obtained results concerning the number of DoF using AIC technique to those obtained using eq. (21). This comparison highlights that the number of DoF for a given UWB channel saturates beyond a certain frequency bandwidth and does not increase linearly. Also an estimation of UWB channel entropy is provided to justify the DoF behavior

12 *R. Saadane et al.*

with respect to the channel bandwidth. Our future work will focus on the study of the evolution of DoF versus the bandwidth for other UWB channels in outdoor, corridors and industrial environments.

## References

- Alomainy, A., Hao, Y., Hu, X., Parini, C. G. and Hall, P. S. [2006] “UWB on-body radio propagation and system modelling for wireless body-centric networks,” *Communications, IEE Proceedings* **153**(1), 107–114.
- Anderson, T. W. [1984] *An Introduction to Multivariate Statistical Analysis*, 2nd edn. (Wiley, New York).
- Bello, P. A. [1963] “Characterization of randomly time-variant linear channels,” *IEEE Trans. Communications Systems* **IC-11**, 360–393.
- Bello, P. A. [1964] “Time-frequency duality,” *IEEE Transactions on Information Theory* **IT-10**, 18–33.
- Cassoli, D., Win, M. Z. and Molish, A. F. [2002] “The ultra-wide bandwidth indoor channel—from statistical model to simulation,” *IEEE Journal on Selected Areas Communications* **2**(2), 1247–1257.
- Federal Communications Commission [2002] “Revision of part 15 of the commissions rules regarding ultra-wideband transmission systems,” *First Report and Order, ET Docket 98153, FCC 0248*; Adopted: February 2002; Released: April 2002.
- Gallagher, R. G. [1968] *Information Theory and Reliable Communication* (Quinn-Woodbine, Inc, United States of America).
- Ganesan, A. and Sayeed, A. M. [2000] “Bandwidth-efficient exploitation of the degrees of freedom in a multipath fading channel,” in *Proc. IEEE International Symposium on Information Theory*, 25–30 June 2000, p. 161.
- Ghassemzadeh, S. S., Jana, R., Rice, C. W., Turin, W. and Tarokh, V. [2004] “Measurement and modeling of an indoor UWB channel,” *IEEE Transactions on Communications* **52**(10), 1786–1796.
- Golay, M. J. E. [1949] “Notes on digital coding,” *Proc. IRE* **37**, 657.
- Kunisch, J. and Pamp, J. [2002] “Measurement results and modeling aspects for UWB radio channel,” *Proc. of IEEE Conference Ultra Wideband Systems and Technologies*, pp. 19–23.
- Matz, G., Molisch, A. F., Hlawatsch, F., Steinbauer, M. and Gaspard, I. [2002] “On the systematic measurement errors of correlative mobile radio channel sounders,” *IEEE Trans. on Communications*, **50**(5).
- Rappaport, T. S. [1999] *Wireless Communications: Principles and Practice* (Englewood Cliffs, NJ: Prentice-Hall).
- Saadane, R., Menouni, A., Knopp, R. and Aboutajdine, D. [2004] “Empirical eigenanalysis of indoor UWB propagation channels,” *Proc. of IEEE Global Telecommunications Conference*.
- Slepian, D. and Pollak, H. O. [1961] “Prolate spheroidal wave functions, Fourier analysis, and uncertainty-I”, *Bell System Tech. J.* **40**, 43–64.
- Svantesson, T. and Wallace, J. [2002] “Statistical characterization of the indoor MIMO channel based on LOS/NLOS measurements,” *Conference Record of the 36th Asilomar Conference on Signals, Systems and Computers*, pp. 1354–1358.
- Telatar, I. E. and Tse, D. N. C. [2000] “Capacity and mutual information of wideband multipath fading channels,” *IEEE Trans. on Information Theory* **2**(2), 1384–1400.
- Tsuda, K. and Noble, W. S. [2004] “Learning kernels from biological networks by maximizing entropy,” *Bioinformatics* **20**(1), 326–333. DOI: 10.1093/bioinformatics/bth906.

- Van Trees, H. L. [2001] *Detection, Estimation, and Modulation Theory, Part III: Radar/Sonar Signal Processing and Gaussian Signals in Noise*, Chapter 4, "Special Categories of Detection Problems," (John Wiley and Sons, Inc).
- Wax, M. and Kailath, T. [1985] "Detection of signals by information theoretic criteria," *Trans. on Acoustics, Speech, and Signal Processing* **ASSP-33**(2), 387–392.
- Win, M. Z. and Scholtz, R. A. [1998] "Impulse radio: How it works," *IEEE Communications Letters*, **2**(2), 36–38.
- Williams, D. B. [1994] "Counting the degrees of freedom when using AIC and MDL to detect signals," *IEEE Trans. on Signal Processing* **42**(11).
- Wozencraft, J. M. and Jacobs, I. M. [1965] *Principles of Communication Engineering* (John Wiley and Sons, Reprinted by Waveland Press).
- Xu, G., Roy, III R. H. and Kailath, T. [1994] "Detection of number of sources via exploitation of centro-symmetry property," *IEEE Trans. on Acoustics, Speech, and Signal Processing* **ASSP-42**(1), 102–112.